# Selective Adsorption of Lattice Peptides on Patterned Surfaces

Adam Swetnam and Michael P. Allen
*Department of Physics, University of Warwick, Coventry CV4 7AL, United Kingdom*
(Dated: June 2, 2012)

To study the adsorption of individual peptides in implicit solvent, we propose a version of the Wang-Landau Monte Carlo algorithm that uses a single surface, with no need for a confining wall or grafting. The new "wall-free" method is both more efficient than the traditional ones, and free of additional assumptions or approximations. We illustrate it by simulating an HP-model lattice peptide on planar surfaces with a variety of patterns of adsorption sites, discovering a temperature-induced switch of surface selection which is due to a balance of energetic and entropic effects.

PACS numbers: 87.14.et,87.15.ak,87.15.Zg,05.10.Ln

Understanding the way in which biomolecules such as proteins and peptides bind selectively to mineral surfaces is crucial to a range of applications in nanotechnology [1–3] and bio-inspired materials design [4–6]. Molecular simulations give valuable insight into surface selectivity in peptides [7–10] suggesting causes such as charge, side-group chemistry, solvent structure, and surface epitaxy, which may be tested directly against experimental observations. More idealized, coarse-grained, models have the complementary task of identifying trends and revealing regions of parameter space in which "interesting" behavior, such as a switch in adsorption preference, occurs. By extracting such information from these more economical and extensive, simulations, we may hope to derive general principles for novel materials design. In this paper we propose an improved method for studying adsorption, which we illustrate by studying one exemplary peptide against a wide range of patterned surfaces, discovering a purely temperature-induced switch in selectivity.

Coarse-grained peptide and protein models frequently treat the solvent implicitly [11–13], and we restrict our interest to this case. For illustration, we adopt the simplest peptide model available, the HP model [14]. This is defined as a chain of monomers on a simple cubic lattice of unit spacing; each site is either occupied by a single monomer bead, or is considered to contain solvent. Successive monomers in the chain occupy adjacent sites, and chain crossings are not allowed. The effects of solvent quality and temperature are represented by an interaction energy $-\epsilon$ between nearest-neighbor non-bonded beads. The monomers are of two kinds, H and P: only the H (hydrophobic) beads interact in this way. Interactions between the P (polar) beads, between H and P beads, and all solvent interactions, are considered to be integrated out of the problem. This model has been described as the "Ising model" of protein simulation [15]. Throughout this paper we shall consider only a single peptide chain of this kind, examining its behavior in great detail.

The planar surface of adsorption is defined by $z = 0$, with peptide monomers restricted to $z > 0$. Interactions between the peptide and the surface again involve only nearest-neighbor lattice sites. The strength of the surface interaction will be denoted $\sigma$; we allow surface sites to be either interacting or non-interacting, according to a specified two-dimensional periodic pattern, and moreover to interact with either, or both, types of bead. $\Gamma$ will represent both the internal conformation and the overall $(x, y)$ position of the peptide (which is only significant modulo the periodicity of the pattern of adsorption sites in the surface). Let $n_\Gamma$ be the number of internal H-H contacts, and $s_\Gamma$ the number of surface interactions, in state $\Gamma$; then the peptide energy is $E_\Gamma = -n_\Gamma\epsilon - s_\Gamma\sigma$, given that it is in contact with the surface.

Our goal is to obtain the adsorption behavior for a given peptide against a given patterned surface as a function of $\epsilon$, $\sigma$ and temperature $T$ in the most efficient manner possible, and then compare different surfaces against one another. We achieve this by determining the density of states $W(n, s)$ of the adsorbed peptide, which is proportional to the number of states $\Gamma$ having specified numbers of contacts $n_\Gamma = n$ and $s_\Gamma = s$. The Wang-Landau Monte Carlo simulation method [16] allows a determination of $W(n, s)$ from a single Monte Carlo run. The essential element is the replacement of the Boltzmann factor in the conventional Monte Carlo acceptance criterion by the ratio $W^{\rm old}/W^{\rm new}$, resulting in an asymptotic distribution of states $\Gamma$ with a density proportional to the *inverse* of $W$. $W$ is initially set equal to 1 everywhere, and the value of $W$ at each visited point $(n, s)$ is modified according to $W \to {\rm e}^\phi W$: this tends to result in *uniform* sampling of the values $(n, s)$ as the simulation proceeds. The modification exponent $\phi$ is progressively reduced $1 \to 0$ using a schedule based on the roughness of the distribution [17–19], resulting in convergence to the desired $W(n, s)$; details are given elsewhere [20]. We use the Monte Carlo move set known as "pull moves" [21], which have been shown to satisfy detailed balance, to be efficient, and ergodic for systems of this type [22, 23]. Typically we conduct 15 independent Wang-Landau simulations, each of length $10^{11}$ moves, for each system.

The novel feature of our study of adsorption thermodynamics is the use of a *single* surface, and the avoidance of directly simulating any desorbed states of the peptide. In principle, the desorbed molecule is free to explore the

infinitely large upper half-space; in other words, the system is unbounded. To counter this, two approaches are in common use [24]. The first is to study a system in which one end of the polymer is permanently "tethered" or "grafted" to the surface [25–28]. This has the disadvantage of being different from the physical system of interest. The more common alternative is to add a second, confining, wall, parallel to the surface of interest [15, 22, 29–31]. This is usually called "slab" or "slit" geometry, and it is also sub-optimal. Firstly, the walls need to be sufficiently separated to avoid interference; in principle the slit width dependence should be studied. Secondly, the desorbed molecule makes long excursions away from the surface, building up values of $W(n, s = 0)$. On re-adsorption, a long period elapses during which attempts to desorb are rejected, until the accumulated deficiency in $W(n, s > 0)$ is rectified. A third source of inefficiency is that a certain fraction of attempted moves will be rejected due to overlap with the surface of interest, or the confining wall.

Our approach [23] avoids these problems. Each MC move can be regarded as being combined with the unique vertical translation that brings the surface into contact with the peptide: overlaps with the surface, and desorbed configurations, never arise. We call these simulations "wall free" because there is no second wall. The essential element is that the density of states is resolved according to $n$ and $s$. For desorbed states, the analogous quantity, defined with respect to internal contacts alone, may be expressed $W_0(n) = \sum_s W(n, s)$. Consequently, both relevant quantities may be determined from a single Wang-Landau run. Partition functions in the constant-temperature ($T$) ensemble, for both adsorbed and desorbed states, are defined

$$Q(T) = \sum_{n,s} W(n, s) \mathrm{e}^{+\beta n \epsilon} \mathrm{e}^{+\beta s \sigma}$$

$$Q_0(T) = \sum_{n,s} W(n, s) \mathrm{e}^{+\beta n \epsilon} = \sum_{n} W_0(n) \mathrm{e}^{+\beta n \epsilon} ,$$

where $\beta = 1/kT$. The free energy, $F = -kT \ln Q$, and all relevant thermodynamic quantities, may be calculated directly for both adsorbed and desorbed states. It is easy to show, for the single-peptide system, that the mean number of molecules per lattice site, which provides a direct measure of the adsorption, satisfies

$$\ln\big(\langle N \rangle / \langle N_0 \rangle\big) = \ln\big(Q/Q_0\big) = -\beta(F - F_0) \, .$$

We have conducted a wide range of simulations of different HP model peptides against a variety of striped and checkerboard patterned surfaces. To illustrate the power of the above strategy to discover a delicate balance between entropic and energetic effects in surface selectivity, we concentrate on a particular 36-bead peptide, the dodecamer $(\mathrm{PHP})_{12}$, and its adsorption on just three of these surfaces. All the surfaces attract only the polar (P) beads

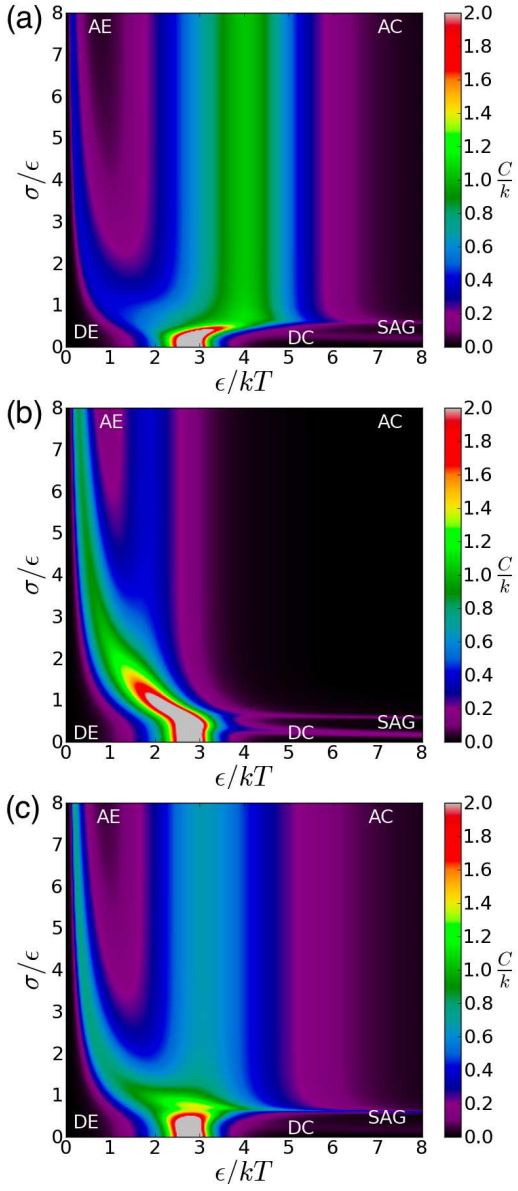


FIG. 1: (Color online) Heat capacity $C$, as a function of inverse temperature $1/kT$ and surface interaction strength $\sigma$, both expressed in terms of internal interaction strength $\epsilon$, for peptide $(\mathrm{PHP})_{12}$ adsorbed on (a) uniform polar surface $P$; (b) checkerboard surface $P_{2\times2}$ and (c) striped surface $P_{3+3}$. The five principal pseudophases are marked and described in the text.

in the peptide: the first, $P$, is uniform, i.e. un-patterned; on the second, $P_{2\times2}$, the attractive and non-attractive sites are arranged in a checkerboard of $2 \times 2$ squares, while on the third, $P_{3+3}$, they appear in parallel stripes, three lattice spacings in width. These might represent, for instance, different facets of a nanoparticle. The peptide $(\mathrm{PHP})_{12}$ has a well-defined ground state in the bulk, comprising a cuboidal $2\times2\times3$ hydrophobic core, shielded almost completely by polar beads [32].

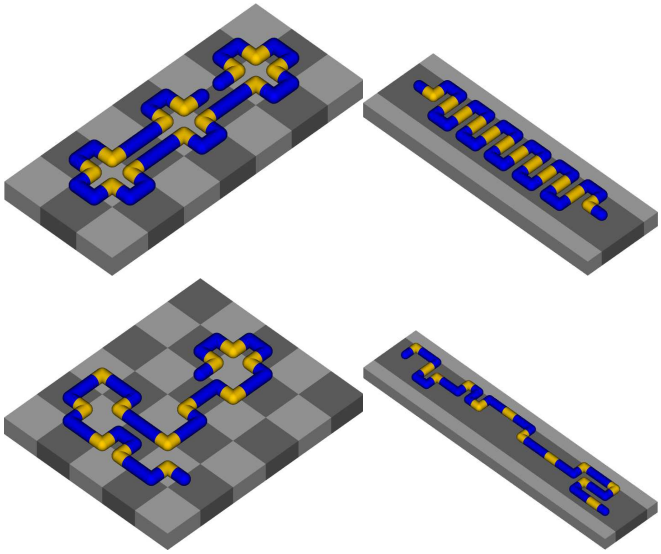

FIG. 2: (Color online) Snapshots of the AC and AE configurations on the patterned surfaces of interest. The peptide is colored blue (polar, P) and yellow (hydrophobic, H); the monomer beads and the bonds between them are given the same radius to aid visualization. Surface sites that are attractive to polar beads are colored dark gray, non-attractive sites light gray. The AC phase on the uniform surface is essentially identical to that on $P_{2\times2}$; the AE phase is similar, but more disordered.

The surface phase diagrams of all three systems, in the form of heat capacity $C$ as a function of inverse temperature and surface strength (both normalized by the internal interaction parameter $\epsilon$) are shown in Fig. 1. Pseudophases are practically identified as regions of low $C$, separated by ridges indicating larger energy fluctuations. (A range of other order parameters and free-energy derivatives also assist in distinguishing the different phases, but here the heat capacity is sufficient). Common features of the phase diagram are the high-temperature desorbed-expanded (DE) phase, which is essentially a self-avoiding random walk in three dimensions, and the low-temperature desorbed-compact (DC) and surface-adsorbed-globule (SAG) phases, in both of which the peptide adopts the ground-state cuboid form [25, 26]. For $\sigma/\epsilon \gtrsim 1$, the adsorbed-compact (AC) and adsorbed-expanded (AE) phases begin to appear. These phases are similar on $P$ and $P_{2\times2}$, but different from $P_{3+3}$, as illustrated in Fig. 2. The AC-AE transition is rather broad in the $P_{3+3}$ case, reflecting the quasi-one-dimensional nature of both phases, which are largely restricted to a single stripe in order to optimise the surface energy. The formation of a well-defined AE phase occurs at larger $\sigma$ and higher $T$ for $P_{2\times2}$ than for $P$ and $P_{3+3}$, due (as we shall see) to its lower entropy on $P_{2\times2}$.

Comparison of adsorption free energies on the two patterned surfaces (for equal values of $\sigma$) reveals a dramatic

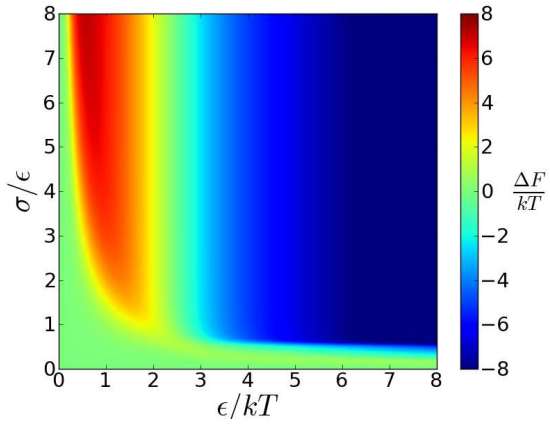


FIG. 3: (Color online) Free energy difference $\Delta F = F(P_{2\times2}) - F(P_{3+3})$ of peptide $(\mathrm{PHP})_{12}$ as a function of inverse temperature $\epsilon/kT$ and surface strength $\sigma/\epsilon$.

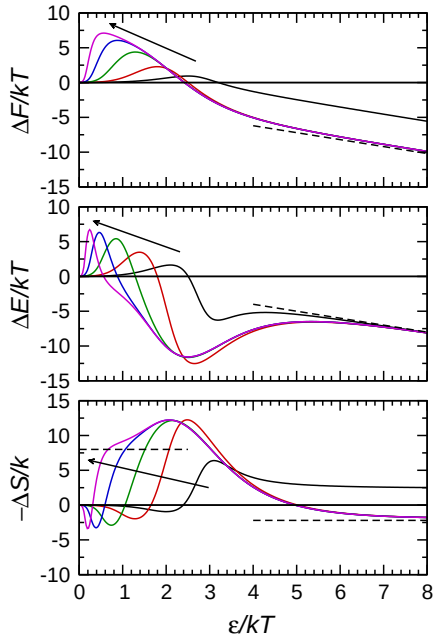


FIG. 4: (Color online) Free energy, internal energy, and (negative) entropy of peptide adsorbed on checked $P_{2\times2}$ surface relative to striped $P_{3+3}$ surface. Surface strength (increasing values indicated by arrows): $\sigma/\epsilon = 0.5$ (black), 1.0 (red), 2.0 (green), 4.0 (blue), 8.0 (magenta). The dashed lines represent the limiting behavior at low and high temperature (see text).

effect. In Fig. 3, it can be seen that a switch in thermodynamic stability (and hence relative adsorption) occurs, at the approximate temperature $kT/\epsilon \approx 0.4$ of the AE-AC phase transition, for all values of $\sigma/\epsilon \gtrsim 1$. This switch is due to a balance between energetic and entropic terms, which is quantified in Fig. 4, and can be understood in part by examining the associated AC and AE configurations in Fig. 2. The AC phase has a lower energy on the checked surface: $E(P_{2\times2}) = -24\sigma - 12\epsilon$, compared with $E(P_{3+3}) = -24\sigma - 11\epsilon$. The net energy

difference $\Delta E = E(P_{2\times2}) - E(P_{3+3}) = -\epsilon$ increasingly favors $P_{2\times2}$ at low temperature (see Fig. 4). The absolute entropy of both phases may also be calculated exactly, from the number of valid configurations. On $P_{2\times2}$, there are six degenerate arrangements (two linear, and four L-shaped) of the three 12-bead PHP-quartet motifs. Each of these has 12 positions for the two end-beads, giving a total degeneracy of 72. On $P_{3+3}$, there are two equivalent ways of orienting the zig-zag structure along the stripe, and two possible positions for each of the end-beads, giving an overall degeneracy of 8. The net entropy term $\Delta S = S(P_{2\times2}) - S(P_{3+3}) = k\ln(9)$ also favors the checked surface, but the effect is relatively small in comparison with the energetics at low $T$. These contributions are indicated in Fig. 4.

At higher temperatures, $\epsilon/kT \lesssim 2.5$, the situation is quite different. In this regime, the AE phase has slightly lower energy on $P_{3+3}$ as there are more opportunities for H-H contacts. More significantly, the entropy difference strongly favors $P_{3+3}$. Figure 2 shows that, for $P_{2\times2}$, the polar beads trace a path along the edges of the squares: at each corner the intervening hydrophobic bead has a choice of two equivalent sites, and each adjacent polar dimer has a choice of two directions. For $(\mathrm{PHP})_{12}$, ignoring the non-overlap constraint and any effect of the H-H interactions, this gives $S(P_{2\times2})/k = 24\ln 2 \approx 16.6$ which is very close to the value calculated in our simulations. In comparison, $S(P_{3+3})/k \approx 24.6$, similar to that of a self-avoiding random walk confined to a strip [33]. The net $\Delta S = S(P_{2\times2}) - S(P_{3+3}) \approx -8k$ strongly favors the striped surface, and this is indicated in Fig. 4. As can be seen in the figure, these approximate calculations oversimplify the situation: the entropy difference reaches higher values than this, probably because of the large fluctuations associated with the AE-AC phase transition on $P_{3+3}$, and because the AE phase on $P_{2\times2}$ does not become properly established until $\sigma/\epsilon \gtrsim 4$ (see Fig. 1). The energy and entropy effects combine in such a way that the free energies become equal at a temperature which is almost independent of $\sigma/\epsilon$ (except at the lowest values, where there is little adsorption).

Although we find this temperature-induced switch between surfaces to be uncommon for this peptide, it is not unique. We observe a similar $\Delta F$ landscape for $P_{2\times2}$ relative to the uniform $P$ surface, if the surface attraction strength of the latter is reduced by about 10% relative to $P_{2\times2}$. Although the AC structures are identical, the reduction in $\sigma$ disfavors the uniform surface; for the AE phase, however, it becomes strongly favored by entropy.

We have illustrated the "wall-free" approach with a simple lattice model, but it may be generalized to the off-lattice case, in the absence of explicit solvent. Provided the surface-peptide interaction is of finite range, it should be possible to resolve the adsorbed density of states according to separate internal and surface energies, and to express the density of states and partition function of the desorbed state in terms of these. Unlike traditional slit and end-grafted methods, the wall-free method computes single-peptide adsorption thermodynamics directly, without additional approximations or assumptions.

Computer facilities were provided by the Centre for Scientific Computing at the University of Warwick. This work was supported by the Engineering and Physical Sciences Research Council (through a studentship to ADS and grant number EP/I001514/1). This programme grant funds the Materials Interface with Biology (MIB) consortium.

[1] C. Tamerler and M. Sarikaya, ACS Nano **3**, 1606 (2009).
[2] J. M. Slocik and R. R. Naik, Chem. Soc. Rev. **39**, 3454 (2010).
[3] U. O. S. Seker and H. V. Demir, Molecules **16**, 1426 (2011).
[4] R. A. Metzler, J. S. Evans, C. E. Killian, D. Zhou, T. H. Churchill, N. P. Appathurai, S. N. Coppersmith, and P. U. P. A. Gilbert, J. Am. Chem. Soc. **132**, 6329 (2010).
[5] C. B. Ponce and J. S. Evans, Cryst. Growth Des. **11**, 4690 (2011).
[6] S. V. Patwardhan, F. S. Emami, R. J. Berry, S. E. Jones, R. R. Naik, O. Deschaume, H. Heinz, and C. C. Perry, J. Am. Chem. Soc. **134**, 6244 (2012).
[7] H. Heinz, B. L. Farmer, R. B. Pandey, J. M. Slocik, S. S. Patnaik, R. Pachter, and R. R. Naik, J. Am. Chem. Soc. **131**, 9704 (2009).
[8] M. Hoefling, F. Iori, S. Corni, and K.-E. Gottschalk, Langmuir **26**, 8347 (2010).
[9] J. Schneider and L. C. Ciacchi, J. Am. Chem. Soc. **134**, 2407 (2012).
[10] L. B. Wright and T. R. Walsh, J. Phys. Chem. C **116**, 2933 (2012).
[11] T. Bereau and M. Deserno, J. Chem. Phys. **130**, 235106 (2009).
[12] M. Cheon, I. Chang, and C. K. Hall, Proteins: Structure Function and Bioinformatics **78**, 2950 (2010).
[13] Y. Wang and G. A. Voth, J. Phys. Chem. B **114**, 8735 (2010).
[14] K. F. Lau and K. A. Dill, Macromolecules **22**, 3986 (1989).
[15] Y. W. Li, T. Wuest, and D. P. Landau, Comput. Phys. Commun. **182**, 1896 (2011).
[16] F. G. Wang and D. P. Landau, Phys. Rev. Lett. **86**, 2050 (2001).
[17] R. E. Belardinelli and V. D. Pereyra, Phys. Rev. E **75**, 046701 (2007).
[18] R. E. Belardinelli and V. D. Pereyra, J. Chem. Phys. **127**, 184105 (2007).
[19] C. Zhou and J. Su, Phys. Rev. E **78**, 046705 (2008).
[20] A. D. Swetnam and M. P. Allen, J. Comput. Chem. **32**, 816 (2011).
[21] N. Lesh, M. Mitzenmacher, and S. Whitesides, in *Proc. 7th Ann. Int. Conf. Research in Computational Molecular Biology*, edited by M. Vingron, S. Istrail, P. Pevzner, and M. Waterman (ACM, New York, 2003), pp. 188–195.
[22] T. Wüst and D. P. Landau, Comput. Phys. Commun. **179**, 124 (2008).

[23] A. D. Swetnam and M. P. Allen, Phys. Chem. Chem. Phys. **11**, 2046 (2009).
[24] M. Moeddel, W. Janke, and M. Bachmann, Macromolecules **44**, 9013 (2011).
[25] T. Vrbová and S. G. Whittington, J. Phys. A Math. Gen. **27**, 3989 (1998).
[26] Y. Singh, D. Giri, and S. Kumar, J. Phys. A Math. Gen. **34**, L67 (2001).
[27] A. L. Owczarek, A. Rechnitzer, J. Krawczyk, and T. Prellberg, J. Phys. A Math. Gen. **40**, 13257 (2007).
[28] J. Luettmer-Strathmann, F. Rampf, W. Paul, and K. Binder, J. Chem. Phys. **128**, 064903 (2008).
[29] M. Bachmann and W. Janke, Phys. Rev. Lett. **95**, 058102 (2005).
[30] M. Bachmann and W. Janke, Phys. Rev. E **73**, 041802 (2006).
[31] M. Radhakrishna, S. Sharma, and S. K. Kumar, J. Chem. Phys. **136**, 114114 (2012).
[32] K. Z. Yue and K. A. Dill, Phys. Rev. E **48**, 2267 (1993).
[33] F. T. Wall, W. A. Seitz, J. C. Chin, and F. Mandel, J. Chem. Phys. **67**, 434 (1977).